Powder Technology 462 (2025) 121139

Contents lists available at ScienceDirect

Powder Technology

journal homepage: www.journals.elsevier.com/powder-technology

Charge induction-based detection of particulate matter concentration: Effects of environmental parameters on measurement accuracy

Shengyong Lu, Kai Zhang, Yaqi Peng *

State Key Laboratory of Clean Energy Utilization, Institute for Thermal Power Engineering, Zhejiang University, Hangzhou 310027, China

HIGHLIGHTS

- A new set of portable particulate matter concentration detection equipment.
- Simulation experiments based on combined wind tunnel test bench.
- Wind speed, temperature and humidity are negatively correlated with error.
- Size is positively correlated with error.
- Different factors have critical values, restrict each other and work together.

GRAPHICAL ABSTRACT

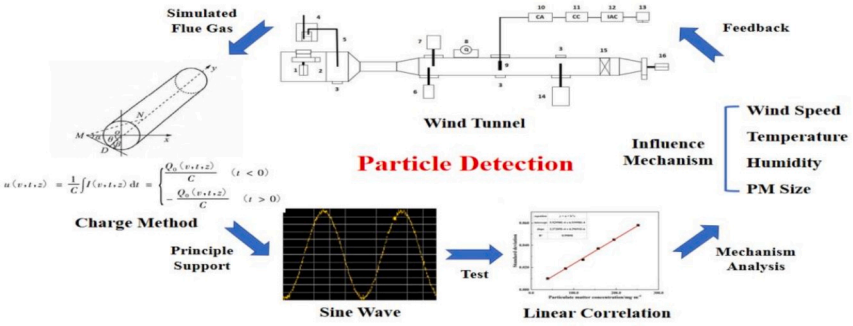

ARTICLE INFO

Keywords:
Particulate matter
Charge
Wind speed
Temperature
Humidity
Size

ABSTRACT

Particulate matter is a primary pollutant generated by waste incineration. This study developed a novel particulate matter concentration detection system based on charge induction principle and investigated the influence of wind speed, temperature, humidity and particle size on measurement accuracy. The detection error decreased with increasing wind speed, temperature, humidity, as well as decreasing particle size. The degree of factors influencing detection accuracy ranked as follows: wind speed > humidity > temperature ≈ particle size. Wind speed primarily affected collision and friction effects and the number of particulate matters passing through the electrode. Temperature and humidity influenced the specific resistance and conductivity of particles, while particle size affected the nucleus-mass ratio and the spatial distribution uniformity at a given mass concentration. This study validates the feasibility of the charge method for particulate matter detection and provides valuable data for the exploration of influencing factors.

1. Introduction

Incineration is one of the effective treatment technologies for municipal solid waste and industrial waste[40,41]. However, the incineration flue gas contains a variety of pollutants, such as VOCs, acidic gases (HCl, SO_x, NO_x etc.), particulate matters, heavy metals and so on[15,16,21,36]. These pollutants cause strong environmental risk on soil, water and organisms once entering the environment[3,30,33,34]. Consequently, pollutant detection and control technologies have emerged as a pivotal research priority within the environmental

* Corresponding author.
E-mail address: pengyaqi@zju.edu.cn (Y. Peng).

https://doi.org/10.1016/j.powtec.2025.121139
Received 15 December 2024; Received in revised form 14 May 2025; Accepted 18 May 2025
Available online 20 May 2025

protection field.

As one of the primary pollutants, particulate matter necessitates real-time concentration monitoring as a critical component of effective emission control strategies. To address the limitation of the traditional weighing method[35,39], such as its slow detection speed and inability to obtain real-time data, new PM concentration detecting technologies have been developed, including laser method[18,19,42], oscillating balance method[31], charge method[8,26,27] and so on. These emerging technologies enable faster, more accurate and real-time monitoring of particulate matters in the flue gas. Notably, the charge detection method demonstrates distinct advantages, including simpler equipment configuration, ease of installation and maintenance, and reduced operational costs. These characteristics render it particularly applicable for PM concentration detection in industrial applications such as mining operations and waste incineration.

The charge-based detection methodology is fundamentally grounded in the principle of electrostatic induction. When particulate matters flow in a confined space such as a pipe, friction and collision occur between particulate matter and either matter or the pipe wall, so that particulate matters acquire a certain amount of positive and negative charge [1,9,10,24]. When the charged particulate matters pass near the metal electrode, the induced electrical signal is measured, which correlates with PM concentration[12,29,44].

Building upon the theoretical framework, detection technology predicated on charge induction principles has been systematically investigated and implemented. The results of Hu et al.[11] proved that the induced and transferred charges can be converted into two independent voltage signals, and the root mean square of the induced charge signal and the slope of the transferred charge signal increase with the mass flow rate and particulate matter velocity. Liu et al.[17] found that the diameter ratio would affect the electrostatic induction effect, and obtained the maximum electrostatic induction under a better diameter ratio. Chen et al.[5] analyzed the influence of the length and width of the electrode and the particle flow rate on the standard deviation of the induction signa, and the mathematical relationship between the standard deviation and concentration was obtained.

During measurement procedures, environmental parameters exert modulatory effects on the generation and propagation of induced charges, thereby compromising the fidelity of detection outcomes. Therefore, it is imperative to conduct systematic investigations into the underlying mechanisms by which environmental parameters modulate the charge characteristics of particulate matter. For example, Mori et al. [20] proposed that the frequent migration of water molecules and ions will lead to effective collisions between ions and particulate matters, thereby expanding the charge distribution of particulate matters. Zheng et al.[45] discovered significant relationships between environmental conditions and particulate matter charging behavior. For particulate matters with a size of 0.73 μm, when the temperature increased from 300 K to 363 K, the charge on the particulate matters increased by 30 %. Additionally, for particulate matters larger than 0.1 μm, increasing the relative humidity from 30 % to 80 % resulted in more than a 50 % increase in charge. Tang et al.[29] also proved that the charge carried by particles increases with the increase of temperature, concentration and particle size. These studies have laid the foundation for subsequent analysis of the influence of environmental parameters on measurement accuracy.

In addition to environmental parameters, the intrinsic physicochemical properties of particulate matter exert a substantial influence on its charge characteristics. Pecherkin et al.[23] found that the amount of charge carried by particulate matter increases with the increase of particulate matter's mass. Rodrigues et al.[25] empirically observed a linear correlation between the net charge of particulate matter and its diameter. Through systematic investigations of starch particulates and protein-based powders, Landauer et al.[14] postulated that the chemical composition of particulate matter exerts a non-negligible influence on its charge characteristics. Collectively, environmental parameters and intrinsic particulate properties synergistically modulate the charge characteristics of particulate matter, thereby affecting the accuracy of charge induction method.

However, the aforementioned studies exhibit certain limitations. For instance, their findings remain predominantly theoretical in nature, lacking experimental validation through detection equipment and pilot-scale systems; additionally, the selected data ranges demonstrate constrained applicability, particularly in the context of waste incineration flue gas. Therefore, this study designed a PM detection device based on the charge induction principle and conducted tests on a wind tunnel apparatus to investigate the influence of wind speed, temperature, humidity, and PM size on detection errors, while analyzing their underlying mechanisms. This research provides data support for the analysis of particulate matter detection errors and device optimization.

2. Materials and methods

2.1. Experimental installations

A wind tunnel test bench was built to provide a flue gas environment. The specific structure was described in details in the previous study[43]. The structure, key components, and partial parameters are detailed in Fig. S1, Table S1, and Table S2 of the supplementary materials. The tunnel was equipped with an electrical heater, a humidifier, a PM sampler and the detection equipment designed in this study. The electrical heater was used for constant temperature heating of flue gas, the humidifier was used for humidifying flue gas, and the sampler was used to obtain the reference PM concentration.

2.2. Detection equipment

The detection equipment consisted of several parts, including a cylindrical metal electrode, a charge amplifier, an information acquisition card, a data processing software, etc. The specific models and functions of these parts were described in the previous study[43]. The main structures of the charge amplifiers and information acquisition cards are detailed in Fig. S2 of the supplementary materials, with their selection and design referencing existing studies[28]. The information acquisition card input the final signal into the computer, which obtained the characteristic value of the sinusoidal voltage signal through the developed specific data processing software, and then calculated PM concentration according to the fitting formulas. These components were connected through data lines, and the charge amplifier was powered by 24v DC. The subsequent calibration methods for the detection device refer to the research findings of De Vito et al.[7], and are not elaborated here.

2.3. Data collection

The data acquisition of this study primarily involved the acquisition of PM concentration and corresponding electrical signals, as well as measurements of wind speed, temperature, humidity, and PM size. The baseline data of PM concentration were obtained by a sampler with weighing method according to Chinese national standard 'The determination of particulates and sampling methods of gaseous pollutants from exhaust gas of stationary source' (GB/T 16157–1996). The electrical signals were obtained by the equipment designed in this study.

Particulate matters came from waste incineration fly ash of the factory, and the size was distinguished by vibrating screens and ultra-fine screens. The standard referenced Chinese national standard 'Industrial woven wire cloth-Technical requirements and tests'(GB/T 17492–2019).

2.4. Experimental procedure

This study focused on the influence of wind speed, temperature, humidity and PM size on the detection error of the charge method. Both

the single variable method and gradient experimental method were employed. The experimental conditions were referred to the typical values found in waste incineration bag cabin, and the particulate matter employed in this study consisted of representative fly ash obtained from a municipal solid waste incineration facility. To ensure the results' relevance and generalizability, experiments were conducted in both low-concentration (10 and 15 mg/m^3) and high-concentration (80 and 100 mg/m^3) environments. Each experiment was repeated three times, and the average value was taken as the final result.

In the wind speed experiment, each test included 11 groups, and the

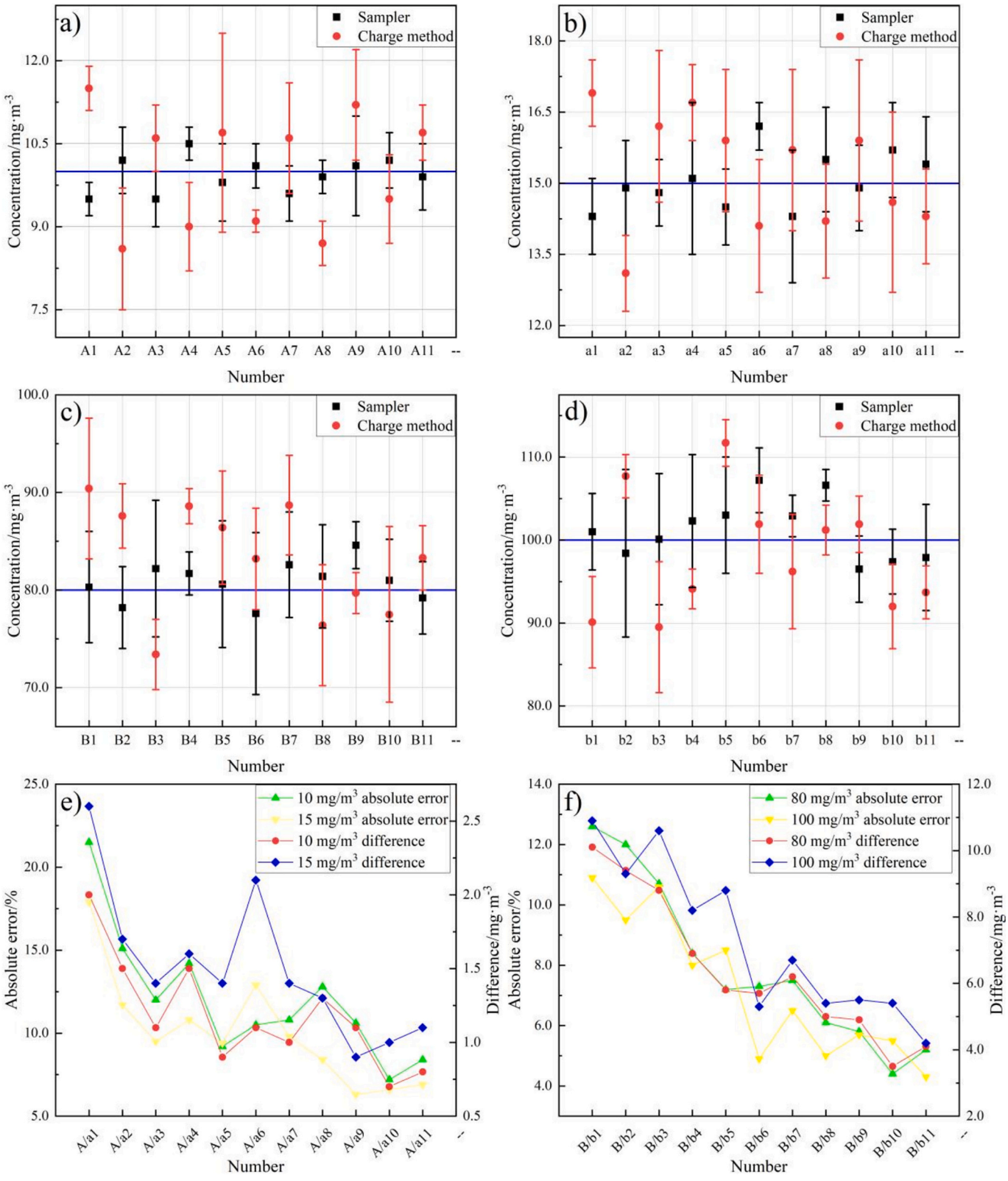

Fig. 1. The results of wind speed at a) 10 mg/m^3, b) 15 mg/m^3, c) 80 mg/m^3, d) 100 mg/m^3 and the error at e) 10 and 15 mg/m^3, f) 80 and 100 mg/m^3.

corresponding wind speed was 0.5 m/s, 0.6 m/s, 0.7 m/s, 0.8 m/s, 0.9 m/s, 1.0 m/s, 1.1 m/s, 1.2 m/s, 1.3 m/s, 1.4 m/s, 1.5 m/s, respectively. All other parameters were held constant, with temperature maintained at ambient conditions (20–25 °C), relative humidity stabilized at 25 %, and particulate matter size distribution confined to the 70–150 μm range.

In the temperature experiment, each test included 8 groups, and the corresponding temperature was 140.0 °C, 150.0 °C, 160.0 °C, 170.0 °C, 180.0 °C, 190.0 °C, 200.0 °C, 210.0 °C, respectively. All other parameters were held constant, with wind speed maintained at 1.0 m/s, relative humidity stabilized at 25 %, and particulate matter size distribution confined to the 70–150 μm range.

In the humidity experiment, each test included 7 groups, corresponding to humidity of 5.0 %, 10.0 %, 15.0 %, 20.0 %, 25.0 %, 30.0 %, 35.0 %, respectively. All other parameters were held constant, with wind speed maintained at 1.0 m/s, temperature stabilized at 160.0 °C, and particulate matter size distribution confined to the 70–150 μm range.

In the size experiment, each test included 9 groups, corresponding to size of 20.0 μm, 30.0 μm, 40.0 μm, 50.0 μm, 60.0 μm, 70.0 μm, 80.0 μm, 90.0 μm, 100.0 μm, respectively. All other parameters were held constant, with wind speed maintained at 1.0 m/s, temperature stabilized at 160.0 °C, and relative humidity controlled at 30.0 %.

3. Results and discussion

3.1. Influence of Wind Speed

The results of wind speed in low-concentration were shown in Fig. 1 a and b. At 10.0 mg/m^3 concentration with 0.5 m/s wind speed, the sampler recorded an average of 9.5 mg/m^3, while the charge method indicated 11.5 mg/m^3, showing the largest discrepancy of 2.0 mg/m^3. When the wind speed increased to 1.4 m/s, the sampler's average value was 10.2 mg/m^3, and the charge method reported 9.5 mg/m^3, with the smallest difference of 0.7 mg/m^3. At 15.0 mg/m^3 concentration with 0.5 m/s wind speed, the sampler recorded 14.3 mg/m^3, and the charge method reported 16.9 mg/m^3, resulting in a 2.6 mg/m^3 difference. At 1.3 m/s wind speed, the sampler's average was 14.9 mg/m^3, and the charge method was 15.9 mg/m^3, showing a reduced difference of 1.0 mg/m^3. The concentration lattice diagram showed that the sampler's results remained consistent near the set value, with minimal deviation, indicating no significant correlation between sampler results and wind speed in the experimental range. However, the charge method results showed greater variance, gradually converging toward the set value as wind speed increased, leading to a reduced difference between the charge method and the sampler.

The results in high-concentration environment were shown in Fig. 1 c and d. At 80.0 mg/m^3 concentration with 0.5 m/s wind speed, the difference between the sampler and charge method was largest, which was 10.1 mg/m^3. When the wind speed increased to 1.4 m/s, the difference showed the smallest discrepancy of 3.5 mg/m^3. At 100.0 mg/m^3 concentration with 0.5 m/s wind speed, the largest difference was 10.9 mg/m^3. At the wind speed of 1.5 m/s, the difference reduced to the smallest value 4.2 mg/m^3. The general rule was similar to the result of low-concentration.

The absolute error of the charge detection method compared to the sampler results were illustrated in Fig. 1 e and f. At 10.0 mg/m^3 concentration, the average absolute error across varying wind speeds was 12.0 %. The maximum error of 21.5 % occurred at a wind speed of 0.5 m/s, while the minimum error of 7.2 % was observed at 1.4 m/s. When the concentration was set to 15.0 mg/m^3, the average absolute error decreased slightly to 10.0 %. The maximum error at this concentration was 17.9 % at 0.5 m/s, and the minimum was 6.3 % at 1.3 m/s. At 80.0 mg/m^3 concentration, the average of absolute error value was 7.9 %. When the wind speed was 0.5 m/s, the maximum absolute error was 12.6 %. The minimum absolute error of 4.4 % occurred at 1.4 m/s wind speed. When the concentration increased to 100.0 mg/m^3, the average of absolute error value decreased to 7.2 %. The maximum error of 10.9 % occurred at 0.5 m/s, and the minimum absolute error was 4.3 % at 1.5 m/s.

The detection results at different concentrations were consistent. It can be considered that in the wind speed range of 0.5–1.5 m/s, as the wind speed increased, the absolute error value of the charge method gradually decreased. This rule was related to the detection principle. With constant PM concentration, when the wind speed increased, the number of particulate matters passing near the electrode increased per unit time. If the average charge of particulate matters was constant, the induced charge on the electrode increased, which led to the enhancement of the output signal[5]. This led to an increase in the signal-to-noise ratio of the output signal (the ratio of the actual electrical signal to the interference signal), resulting in a decrease in the actual error.

In addition, the wind speed also affected the charge of a single particulate matter. Investigators[13] have found that the greater the speed was, the greater the nuclear-to-mass ratio of particulate matters was. Under low wind speed conditions, particulate matter exhibited reduced mobility with diminished collision and friction effects, consequently resulting in suboptimal charging performance. As wind velocity increased, intensified particle motion significantly enhanced inter-particulate friction and collision frequency, thereby substantially improving the charging efficacy. The explanation of Hu et al.[11] and Ali et al.[2] was consistent with the results and inferences of this study.

3.2. Influence of temperature

The results of temperature in low-concentration environment were shown in Fig. 2 a and b. At 10.0 mg/m^3 concentration with 150.0 °C, the sampler recorded an average of 10.4 mg/m^3, while the charge method indicated 8.9 mg/m^3, showing the largest discrepancy of 1.5 mg/m^3. When the temperature increased to 210.0 °C, the sampler's average reading was 9.8 mg/m^3, and the charge method reported 10.4 mg/m^3, with the smallest difference of 0.6 mg/m^3. At 15.0 mg/m^3 concentration with 140.0 °C, the sampler recorded 15.6 mg/m^3, and the charge method reported 13.5 mg/m^3, resulting in a 2.1 mg/m^3 difference. At 200.0 and 210.0 °C, the sampler's average was 15.7 and 14.0 mg/m^3, and the charge method was 14.4 and 15.4 mg/m^3, showing a reduced difference of 1.3 mg/m^3.

At 80.0 mg/m^3 concentration with 140.0 °C, the difference between the sampler and charge method was largest, which was 9.5 mg/m^3. When the temperature increased to 200.0 °C, the difference showed the smallest discrepancy of 5.9 mg/m^3. At 100 mg/m^3 concentration with 150.0 °C, the largest difference was 9.5 mg/m^3. At the temperature of 210.0 °C, the difference reduced to the smallest value 6.2 mg/m^3. The sampler's results remained consistent near the set value, but the charge method results showed greater variance. The rule was similar to the wind speed experiments.

The absolute error of the charge detection method compared to the sampler results were illustrated in Fig. 2 e and f. At 10.0 mg/m^3 concentration, the average absolute error across varying temperature was 11.8 %. The maximum error of 14.7 % occurred at 140.0 °C, while the minimum error of 10.5 % was observed at 190.0 °C. When the concentration was 15.0 mg/m^3, the average absolute error decreased slightly to 10.8 %. The maximum error was 13.6 % at 140.0 °C, and the minimum was 8.5 % at 200.0 °C. At 80.0 mg/m^3 concentration, the average of absolute error value was 8.4 %. When the temperature was 140.0 °C, the maximum absolute error was 11.0 %. The minimum absolute error of 7.2 % occurred at 210.0 °C. When the concentration increased to 100.0 mg/m^3, the average of absolute error value decreased to 7.4 %. The maximum error of 9.7 % occurred at 150.0 °C, and the minimum absolute error was 6.3 % at 210.0 °C. The results were consistent with the existing research results[29,45].

According to the analysis of the detection principle, the influence of temperature on the detection error was mainly related to the specific

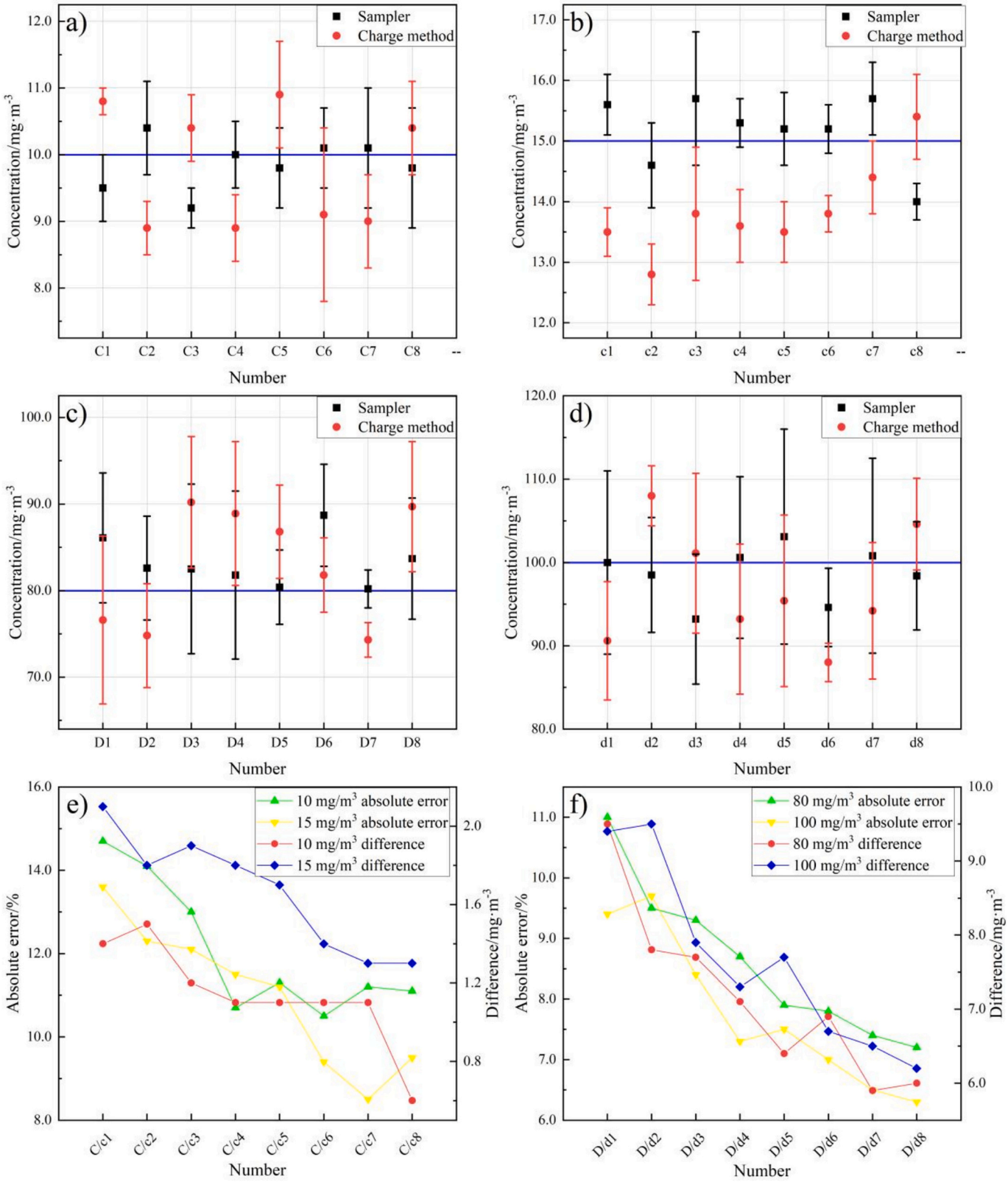

Fig. 2. The results of temperature at a) 10 mg/m^3, b) 15 mg/m^3, c) 80 mg/m^3, d) 100 mg/m^3 and the error at e) 10 and 15 mg/m^3, f) 80 and 100 mg/m^3.

resistance of particulate matters. Miya et al.[22] have proved that the charge of a single particulate was related to temperature. Particulate matters are produced by incineration process, and the components are more complex, usually including carbon-containing compounds, metal compounds, organic compounds, etc. These components cause the specific resistance of particulate matters to change with temperature. For the particulate matters used in this study, as the temperature increased, the surface temperature of particulate matters increased, and the thermal motion intensified[29,45], resulting in the acceleration of internal electronic thermal motion and a decrease in specific resistance,

which improved the charge performance of particulate matters. And this led to a decrease in detection error. However, the increasing temperature gradually reduces the moisture content of particulate matters, and the decrease of moisture content increases the specific resistance, which weakens the influence of the thermal motion strengthening. Therefore, it is not excluded that when the temperature exceeds the experimental range, the detection error increases instead of decreasing.

It was also found that in the four groups, the difference between the maximum and the minimum absolute error was 4.2 %, 5.1 %, 3.8 % and 3.4 %, respectively. In the wind speed experiments, the difference was

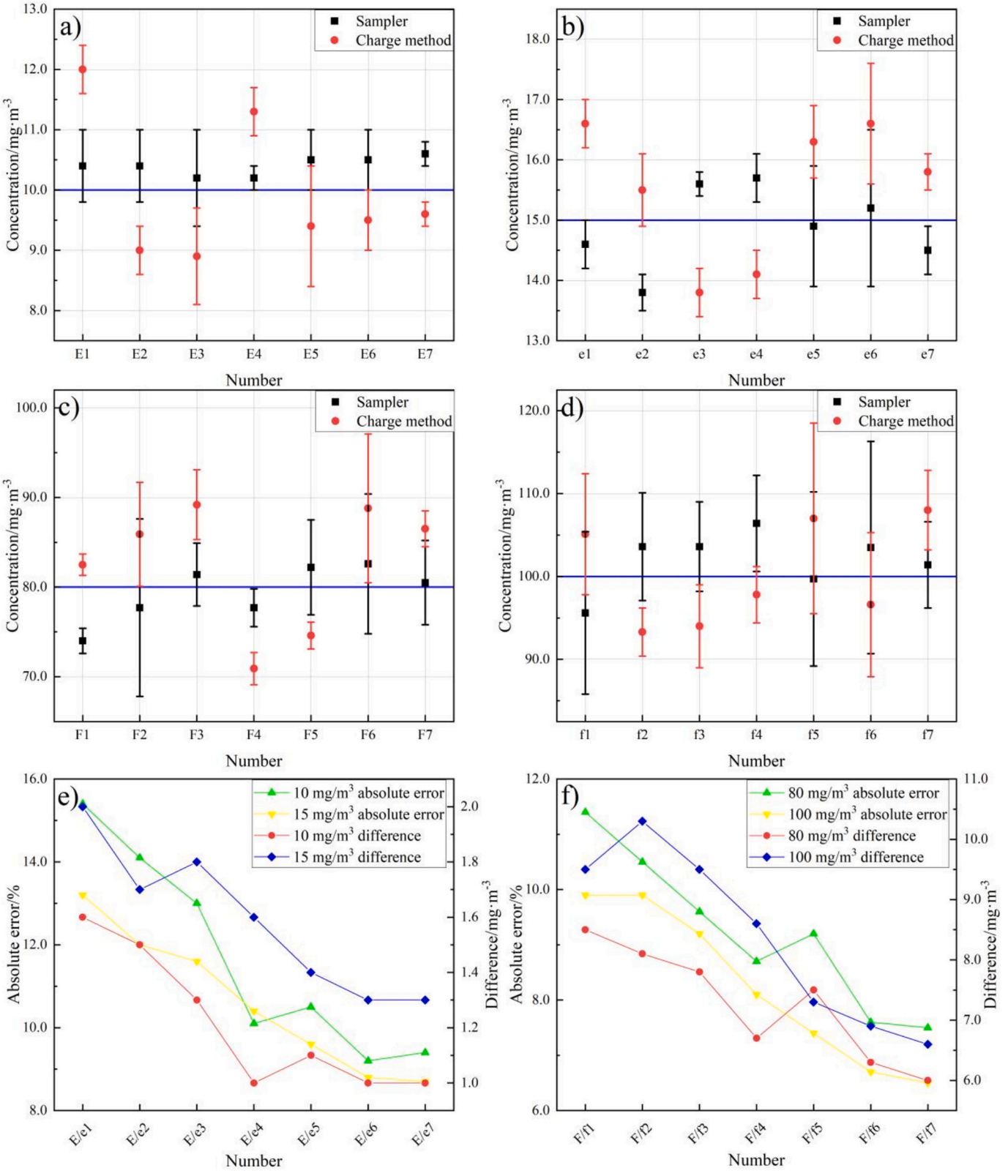

Fig. 3. The results of humidity at a) 10 mg/m^3, b) 15 mg/m^3, c) 80 mg/m^3, d) 100 mg/m^3 and the error at e) 10 mg/m^3 and 15 mg/m^3, f) 80 mg/m^3 and 100 mg/m^3.

14.3 %, 11.6 %, 8.2 % and 6.6 %, respectively. Therefore, it was preliminarily inferred that within the experimental range, the influence of wind speed exceeded that of temperature.

3.3. Influence of humidity

The results of humidity in low-concentration environment were shown in Fig. 3 a and b. At 10.0 mg/m^3 concentration with 5.0 % humidity, the sampler recorded an average of 10.4 mg/m^3, while the charge method indicated 12.0 mg/m^3, showing the largest discrepancy of 1.6 mg/m^3. When the humidity increased to 30.0 %, the sampler's average reading was 10.5 mg/m^3, and the charge method reported 9.5 mg/m^3, with the smallest difference of 1.0 mg/m^3. At 15.0 mg/m^3 concentration with 5.0 % humidity, the sampler recorded 14.6 mg/m^3, and the charge method reported 16.6 mg/m^3, resulting in a 2.0 mg/m^3 difference. At 35.0 % humidity, the sampler's average was 14.5 mg/m^3, and the charge method was 15.8 mg/m^3, showing a reduced difference of 1.3 mg/m^3.

The results in high-concentration environment were shown in Fig. 3 c and d. At 80.0 mg/m^3 concentration with 5 % humidity, the difference between the sampler and charge method was largest, which was 8.5 mg/m^3. When the humidity increased to 35.0 %, the difference showed the smallest discrepancy of 6.0 mg/m^3. At 100 mg/m^3 concentration with 10.0 % humidity, the largest difference was 10.3 mg/m^3. At the humidity of 35.0 %, the difference reduced to the smallest value 6.6 mg/m^3. The sampler's results remained consistent near the set value, but the charge method results showed greater variance. The rule was similar to the previous experiments.

The absolute error of the charge detection method compared to the sampler results were illustrated in Fig. 3 e and f. At 10.0 mg/m^3 concentration, the average absolute error across varying humidity was 11.7 %. The maximum error of 15.4 % occured at 5 % humidity, while the minimum error of 9.2 % was observed at 30 % humidity. When the concentration was 15.0 mg/m^3, the average absolute error decreased slightly to 10.6 %. The maximum error was 13.2 % at 5.0 % humidity, and the minimum was 8.7 % at 35 % humidity. At 80.0 mg/m^3 concentration, the average of absolute error value was 9.2 %. When the humidity was 5,0 %, the maximum absolute error was 11.4 %. The minimum absolute error of 7.5 % occured at 35.0 %. When the concentration increased to 100.0 mg/m^3, the average of absolute error value decreased to 8.2 %. The maximum error of 9.9 % occured at 5.0 % and 10.0 % humidity, and the minimum absolute error was 6.5 % at 35 % humidity.

It could be seen from the above results that within the range of experimental conditions, the detection error of charge method decreased with the increase of humidity. In this study, the set humidity was relatively low, not more than 50 %. In this case, the morphology and size of particulate matters would not change significantly after absorbing water. In the case of other conditions unchanged, when the ambient humidity increased, the content of water molecules in the flue gas increased, and the particulate matters continued to absorb water, causing an increase in water content in PM components. This reduced the specific resistance of particulate matters, thereby enhancing the conductivity and making them easier to carry charge during collision and friction, which made the charge-to-mass ratio increased[45]. Xu et al.[38] also proved that the aquifer formed by particulate matters after absorbing water increased the conductivity and promoted the friction electrification. This led to the enhancement of the electrode induction signal and the improvement of the signal-to-noise ratio of the output signal, which reduced the detection error. Further consideration, there is a saturation value for the absorption of water by particulate matters. When the humidity further increases, the water absorption of particulate matters no longer increases, and the remaining water molecules in the flue gas increase. These water molecules will lead to the reduction of free electrons and ions in the flue gas, thus affecting the charging effect of particulate matters. Therefore, it is not ruled out that when the humidity further increases, the detection error will rise [38,46].

In the four experiments, the difference between the maximum and minimum absolute error was 6.2 %, 4.5 %, 3.9 % and 3.4 %, respectively. The difference was significantly smaller than that of wind speed experiments, and slightly larger than that of temperature experiments. Therefore, it could be preliminarily judged that in this study, the order of the degree of influence on detection error was, wind speed > humidity > temperature. This also showed that concentration and wind speed, which directly affected the number of particulate matters near the electrode, had a greater impact on detection error. Temperature and humidity, which changed the charge performance of particulate matters and then affected the induction signal, had a relatively small impact on detection error.

In general, humidity changed the specific resistance of particulate matters by changing the water content, thus affecting detection error. The rule was that within the range of experimental data, the greater the humidity was, the smaller the detection error was.

3.4. Influence of size

The results of size in low-concentration environment were shown in Fig. 4 a and b. At 10.0 mg/m^3 concentration with 60.0 μm size, the sampler recorded an average of 11.2 mg/m^3, while the charge method indicated 9.8 mg/m^3, showing the largest discrepancy of 1.4 mg/m^3. When the size increased to 20.0 μm, the sampler's average reading was 8.8 mg/m^3, and the charge method reported 9.3 mg/m^3, with the smallest difference of 0.5 mg/m^3. At 15.0 mg/m^3 concentration with 90.0 μm size, the sampler recorded 15.6 mg/m^3, and the charge method reported 13.7 mg/m^3, resulting in a 1.9 mg/m^3 difference. At 20 μm size, the sampler's average was 14.9 mg/m^3, and the charge method was 16.2 mg/m^3, showing a reduced difference of 1.3 mg/m^3. It could be seen that the convergence of the results of charge method was poor, and the difference between charge method and sampler increased firstly and then remained basically stable with the increase of size.

The results in high-concentration environment were shown in Fig. 4 c and d. At 80.0 mg/m^3 concentration with 90.0 μm size, the difference between the sampler and charge method was largest, which was 10.1 mg/m^3. When the size decreased to 20.0 μm, the difference showed the smallest discrepancy of 6.6 mg/m^3. At 100.0 mg/m^3 concentration with 100.0 μm size, the largest difference was 11.3 mg/m^3. At the size of 20.0 μm, the difference reduced to the smallest value 6.5 mg/m^3. The change rule of difference was consistent with that at low-concentration.

The absolute error of the charge detection method compared to the sampler results were illustrated in Fig. 4 e and f. At 10.0 mg/m^3 concentration, the average absolute error across varying size was 12.6 %. The maximum error of 13.4 % occured at a size of 100.0 μm, while the minimum error of 1.7 % was observed at 20.0 μm size. When the concentration was set to 15.0 mg/m^3, the average absolute error decreased slightly to 11.4 %. The maximum error at this concentration was 12.7 % at 100.0 μm size, and the minimum was 9.2 % at 20.0 μm. At 80.0 mg/m^3 concentration, the average of absolute error value was 10.2 %. When the size was 90.0 μm, the maximum absolute error was 12.0 %. The minimum absolute error of 8.1 % occured at 20.0 μm size. When the concentration increased to 100.0 mg/m^3, the average of absolute error value decreased to 8.9 %. The maximum error of 10.8 % occured at 100.0 μm size, and the minimum absolute error was 6.7 % at 20.0 μm size. The data showed that the absolute error increased with the increase of size, and the law was more obvious after the concentration increased.

In general, in a set of experiments, the detection error increased with the increase of size, and the increasing extent didn't change significantly. At the same time, in the four groups, with the increase of concentration, the difference between the maximum and minimum absolute error tended to increase. This showed that compared with low-concentration, the influence of size on the detection error was more obvious at high-concentration. The principle of this law could be

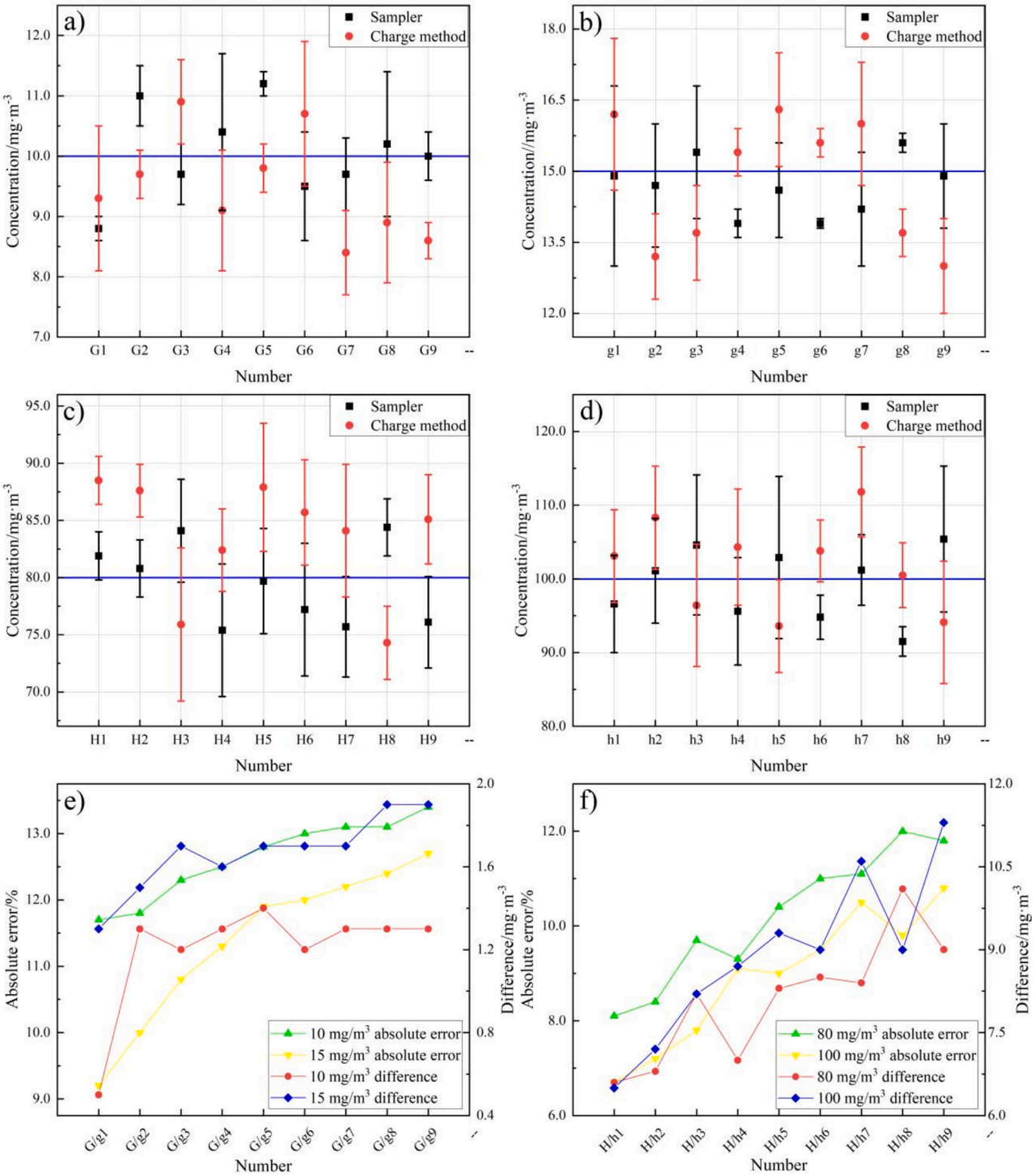

Fig. 4. The results of size at a) 10 mg/m^3, b) 15 mg/m^3, c) 80 mg/m^3, d) 100 mg/m^3 and the error at e) 10 and 15 mg/m^3, f) 80 and 100 mg/m^3.

explained in three aspects. Firstly, when the size was small, the number of particulate matters was more at the same mass concentration, which increased the probability of mutual collision and friction. This greatly improved the charge effect, thus enhancing the induced electrical signal and improving the signal-to-noise ratio of the output signal. Secondly, although small size led to a reduction in the charge of a single particulate matter, it increased the charge-to-mass ratio of particulate matters, that was, the charge capacity of per unit volume was improved[13,22,32]. Cruise et al.[6] also found that the saturated surface charge density was inversely proportional to size. Based on the fact that the output electrical signal was the superposition of the induced electrical signals of each particulate matter, the decrease of size was beneficial to the increase of the charge of the whole PM group, thus enhancing the effective output signal. Furthermore, when the number of particulate matters increased,

the spatial distribution in the tunnel was more uniform, which made the concentration near the electrode closer to the theoretical average, and reduced the accidental error caused by the uneven distribution of particulate matters.

In general, the size affected the error by affecting the charge performance and spatial distribution of particulate matters. The specific law was that within the experimental range, the larger the size was, the greater the detection error was.

In the four experiments of size, the difference between the maximum and minimum absolute error was 1.7 %, 3.5 %, 3.9 % and 4.1 %, respectively. The variation range of the difference was obviously smaller than that of wind speed, and close to temperature. It was considered that the order of influence on detection error was wind speed>humidity>temperature≈size in this study. This conclusion can be explained through the detection principle of the charge method. The charge method is based on the principle of electrostatic induction. As the induced charge quantity increases, the effective electrode signal strengthens, thereby enhancing the system's anti-interference capability and reducing detection errors. Among the four parameters, wind speed directly affects the charging effect of particulate matter and particulate flux, playing a dominant role in determining the magnitude of induced charges. Increased humidity improves particulate conductivity, which is beneficial to the generation and conduction of induced charges. The influence of temperature on particulate conductivity depends on the particulate composition. When particulates contain components with both positive and negative correlations between conductivity and temperature, this weakens the temperature's overall effect. When particle sizes are generally small, their impact on the total induced charge is limited to altering the charge-to-mass ratio of particulates to some extent, resulting in a weaker influence compared to wind speed. Several research findings[4,37] can corroborate the above analysis.

4. Conclusions

This study investigated the influence patterns of wind speed, temperature, humidity, and size on detection errors of charge method. Under the four concentrations of 10 mg/m^3, 15 mg/m^3, 80 mg/m^3, 100 mg/m^3, the order of the degree of influence was wind speed > humidity > temperature ≈ size. Wind speed influenced both the intensity of particle collisions/friction and the particulate flux through the detection electrode. Measurement errors demonstrated an inverse relationship with wind velocity, showing minimum values of 7.2 %, 6.3 %, 4.4 %, and 4.3 %, while maximum errors reached 21.5 %, 17.9 %, 12.6 %, and 10.9 % across tested conditions. Temperature affected the specific resistance of particulate matters. The higher the temperature was, the smaller the error was, but the magnitude of error reduction was shrinking with the increase of temperature. The minimum error was 11.1 %, 8.5 %, 7.2 %, 6.3 %. The maximum error was 14.7 %, 13.6 %, 11.0 %, 9.7 %. Humidity affected the specific resistance of particulate matters. The higher the humidity was, the smaller the error was. And there was a critical value of saturated water absorption. The minimum error was 9.2 %, 8.7 %, 7.5 % and 6.5 %. The maximum error was 15.4 %, 13.2 %, 11.4 %, 9.9 %. Size affected the nuclear-to-mass ratio and the spatial distribution at the same mass concentration. The larger the size was, the greater the error was. The minimum error was 11.7 %, 9.2 %, 8.1 %, 6.7 %. The maximum error was 13.4 %, 12.7 %, 12.0 %, 10.8 %. This study provided an innovative new equipment for detection of particulate matter concentration by charge induction principle and data support for exploration of influencing factors. However, there were still some shortcomings in experimental gradient division, experimental condition setting and principle analysis. Future research will address the aforementioned limitations and focus on establishing a correction system to mitigate the effects of various parameters on detection accuracy.

CRediT authorship contribution statement

Shengyong Lu: Visualization, Investigation, Data curation, Conceptualization. **Kai Zhang:** Writing – review & editing, Writing – original draft, Methodology, Conceptualization. **Yaqi Peng:** Writing – review & editing, Supervision, Methodology, Conceptualization.

Declaration of competing interest

The authors declare that they have no known competing financial interests or personal relationships that could have appeared to influence the work reported in this paper.

Acknowledgements

This work was financially supported by the "Pioneer" and "Leading Goose" R&D Program of Zhejiang (2023C03125).

Appendix A. Supplementary data

Supplementary data to this article can be found online at https://doi.org/10.1016/j.powtec.2025.121139.

Data availability

Data will be made available on request.

References

[1] I.E. Achouri, T. Zeghloul, K. Medles, G. Richard, L. Dascalescu, Factors influencing the triboelectric charging of granular plastics in a rotating-cylinder-type Tribocharger, IOP Conferen. Series: Materi. Sci. Eng. 724 (1) (2020) 012048, https://doi.org/10.1088/1757-899x/724/1/012048.
[2] M. Ali, M. Ghadiri, Analysis of triboelectric charging of particles due to aerodynamic dispersion by a pulse of pressurised air jet, Adv. Powder Technol. 28 (10) (2017) 2735–2740, https://doi.org/10.1016/j.apt.2017.07.026.
[3] H.-J. Bae, J.E. Kang, Y.-R. Lim, Assessment of relative asthma risk in populations living near incineration facilities in Seoul, Korea, Int. J. Environ. Res. Public Health 17 (20) (2020) 7448, https://doi.org/10.3390/ijerph17207448.
[4] L. Ceresiat, H. Grosshans, M.V. Papalexandris, Powder electrification during pneumatic transport: the role of the particle properties and flow rates, J. Loss Prev. Process Ind. 58 (2019) 60–69, https://doi.org/10.1016/j.jlp.2019.01.010.
[5] J. Chen, D. Li, G. Liu, Y. Li, A. Zhang, S. Lu, M. Zhou, Development of a coal dust concentration sensor based on the electrostatic induction method, ACS Omega 8 (14) (2023) 13059–13067, https://doi.org/10.1021/acsomega.3c00319.
[6] R.D. Cruise, S.O. Starr, K. Hadler, J.J. Cilliers, Triboelectric charge saturation on single and multiple insulating particles in air and vacuum, Sci. Rep. 13 (1) (2023) 15178, https://doi.org/10.1038/s41598-023-42265-0.
[7] S. De Vito, G. D'Elia, S. Ferlito, G.D. Francia, M.D. Davidović, D. Kleut, D. Stojanović, M. Jovašević-Stojanović, A global multiunit calibration as a method for large-scale IoT particulate matter monitoring systems deployments, IEEE Trans. Instrum. Meas. 73 (2024) 1–16, https://doi.org/10.1109/tim.2023.3331428.
[8] D. Grondin, P. Breuil, J.P. Viricelle, P. Vernoux, Development of a particulate matter sensor for diesel engine, Procedia Engineering 120 (2015) 1237–1240, https://doi.org/10.1016/j.proeng.2015.08.838.
[9] S. Han, J. Kim, S.H. Ko, Advances in air filtration technologies: structure-based and interaction-based approaches, Materials Today Advances 9 (2021) 100134, https://doi.org/10.1016/j.mtadv.2021.100134.
[10] L.C.J. Heijmans, S. Nijdam, Triboelectric and plasma charging of microparticles, EPL (Europhys. Lett.) 114 (6) (2016) 64004, https://doi.org/10.1209/0295-5075/114/64004.
[11] Y. Hu, Y. Yan, X. Qian, W. Zhang, A comparative study of induced and transferred charges for mass flow rate measurement of pneumatically conveyed particles, Powder Technol. 356 (2019) 715–725, https://doi.org/10.1016/j.powtec.2019.09.006.
[12] G.G. Jang, A.I. Wiechert, Y.-H. Kim, A.P. Ladshaw, T. Spano, J. McFarlane, K. Myhre, J.J. Song, S. Yiacoumi, C. Tsouris, Charging of radioactive and environmental airborne particles, J. Environ. Radioact. 248 (2022) 106887, https://doi.org/10.1016/j.jenvrad.2022.106887.
[13] L. Juan, F. Yu, L. Qiangqiang, W. Bin, W. Jianbo, C. Haiyan, Charging characteristics of sulfur powder in elbow of pneumatic conveying system, IOP Conference Series: Earth and Environmental Science 358 (5) (2019) 052064, https://doi.org/10.1088/1755-1315/358/5/052064.
[14] J. Landauer, S.M. Tauwald, P. Foerst, A simple μ-PTV setup to estimate single-particle charge of Triboelectrically charged particles, Front. Chem. 7 (2019) 323, https://doi.org/10.3389/fchem.2019.00323.

[15] Y. Li, R. Zhao, H. Li, W. Song, H. Chen, Feasibility analysis of municipal solid waste incineration for harmless treatment of potentially virulent waste, Sustainability 15 (21) (2023) 15379, https://doi.org/10.3390/su152115379.
[16] W. Liao, X. Zhang, Z. Fu, S. Zhang, J. Shao, H. Yang, X. Wang, H. Chen, Emission characteristics of typical gas pollutants during oxygen-enriched waste incineration process, Environ. Technol. Innov. 32 (2023) 103358, https://doi.org/10.1016/j.eti.2023.103358.
[17] D. Liu, M. Jing, D. Li, J. Wang, C. Tang, W. Ma, Research on optimization of dust measurement pipeline based on Bernoulli effect, J. Phys. Conf. Ser. 1300 (1) (2019) 012035, https://doi.org/10.1088/1742-6596/1300/1/012035.
[18] S. Molaie, P. Lino, Theoretical Design of the Scattering-Based Sensor for analysis of the vehicle tailpipe emission, Micromachines 11 (12) (2020) 1085, https://doi.org/10.3390/mi11121085.
[19] S. Molaie, P. Lino, Review of the newly developed, Mobile optical sensors for real-time measurement of the atmospheric particulate matter concentration, Micromachines 12 (4) (2021) 416, https://doi.org/10.3390/mi12040416.
[20] T. Mori, Y. Ishii, A. Iwata, T. Okuda, Seasonal charge distributions of submicron atmospheric particles in Yokohama, Japan, Atmos. Environ. 324 (2024) 120421, https://doi.org/10.1016/j.atmosenv.2024.120421.
[21] D. Olejnik, M. Krupa, Selected thermal waste treatment plants in Europe, case study, Civil Environ. Eng. Reports 33 (3) (2023) 1–18, https://doi.org/10.59440/ceer/175240.
[22] S. Omiya, A. Sato, K. Kosugi, S. Mochizuki, Estimation of the electrostatic charge of individual blowing-snow particles by wind tunnel experiment, Ann. Glaciol. 52 (58) (2017) 148–152, https://doi.org/10.3189/172756411797252167.
[23] V.Y. Pecherkin, L.M. Vasilyak, S.P. Vetchinin, V.A. Panov, Limit charge of particulates at their ejection from plane electrode, J. Phys. Conf. Ser. 653 (2015) 012152, https://doi.org/10.1088/1742-6596/653/1/012152.
[24] J. Pérez-Vaquero, M.A.S. Quintanilla, A. Castellanos, Electric charge limits on settled powders, J. Appl. Phys. 119 (22) (2016) 223302, https://doi.org/10.1063/1.4953649.
[25] M.V. Rodrigues, W.D. Marra, R.G. Almeida, J.R. Coury, Measurement of the electrostatic charge in airborne particles: ii -particle charge distribution of different aerosols, Braz. J. Chem. Eng. 23 (1) (2017) 125–133, https://doi.org/10.1590/S0104-66322006000100014.
[26] A. Rostedt, J. Keskinen, Flow rate-independent electrical aerosol sensor, Aerosol Sci. Technol. 52 (11) (2018) 1283–1292, https://doi.org/10.1080/02786826.2018.1498586.
[27] A. Rostedt, M. Marjamäki, J. Yli-Ojanperä, J. Keskinen, K. Janka, V. Niemelä, A. Ukkonen, Non-collecting electrical sensor for particle concentration measurement, Aerosol Air Qual. Res. 9 (4) (2009) 470–477, https://doi.org/10.4209/aaqr.2009.03.0023.
[28] S. Tabandeh, A.P. Vedurmudi, H. Söderblom, S. Pourjamal, P. Harris, Y. Luo, M. Gruber, M. Vaa, M. Johansen, M. Koval, P.F. Østergaard, K. Milicevic, M. A. Zaidan, T. Hussein, T. Petäjä, M. Iturrate-Garcia, M. Davidović, M. van Dijk, G. Kok, A. Xhonneux, A. Merlone, J.A. Sousa, J. Pearce, Sensor network metrology: current state and future directions, Measurement: Senso. 101798 (2025), https://doi.org/10.1016/j.measen.2024.101798.
[29] D. Tang, Z. Ju, L. Wang, Simulation and experimental research on the charged characteristics of particulate matter in the sensor under different exhaust states, Sensors 20 (21) (2020) 6226, https://doi.org/10.3390/s20216226.
[30] P.S. Thind, A. Sareen, D.D. Singh, S. Singh, S. John, Compromising situation of India's bio-medical waste incineration units during pandemic outbreak of COVID-19: associated environmental-health impacts and mitigation measures, Environ. Pollut. 276 (2021) 116621, https://doi.org/10.1016/j.envpol.2021.116621.
[31] Y. Tu, R. Tong, Q. Li, Study on dust measurement technology by oscillating balance method, IOP Conference Series: Earth and Environmental Science 440 (4) (2020) 042072, https://doi.org/10.1088/1755-1315/440/4/042072.
[32] R.S. Vaddi, Y. Guan, I. Novosselov, Behavior of ultrafine particles in electro-hydrodynamic flow induced by corona discharge, J. Aerosol Sci. 148 (2020) 105587, https://doi.org/10.1016/j.jaerosci.2020.105587.
[33] R. Wan, J. Wu, J. Guo, J. Qu, L. Li, L. Tang, Baseline soil dioxin levels from sites where municipal solid waste incineration construction is planned throughout China: characteristics, Sources and Risk Assessment, Sustainability 15 (12) (2023) 9310, https://doi.org/10.3390/su15129310.
[34] G. Wang, K. Huang, Q. Fu, J. Chen, J. Huo, Q. Zhao, Y. Duan, Y. Lin, F. Yang, W. Zhang, H. Li, J. Xu, X. Qin, N. Zhao, C. Deng, Response of PM2.5-bound elemental species to emission variations and associated health risk assessment during the COVID-19 pandemic in a coastal megacity, J. Environ. Sci. 122 (2022) 115–127, https://doi.org/10.1016/j.jes.2021.10.005.
[35] Y. Wang, B. Wang, R. Wang, Current status of detection Technologies for Indoor Hazardous air Pollutants and Particulate Matter, Aerosol Air Qual. Res. 23 (12) (2023) 230193, https://doi.org/10.4209/aaqr.230193.
[36] C. Wei, Y. Zhang, X. Zuo, C. Wan, Z. Wang, Assessment of Zn, Pb and cd in soil around an MSW incineration plant: using risk assessment and multivariate statistical techniques, Processes 11 (11) (2023) 3175, https://doi.org/10.3390/pr11113175.
[37] L. Xie, J. Li, Y. Liu, Review on charging model of sand particles due to collisions, Theor. Appl. Mech. Lett. 10 (4) (2020) 276–285, https://doi.org/10.1016/j.taml.2020.01.047.
[38] W. Xu, H. Grosshans, Experimental study of humidity influence on triboelectric charging of particle-laden duct flows, J. Loss Prev. Process Ind. 81 (2023) 104970, https://doi.org/10.1016/j.jlp.2022.104970.
[39] Y. Yang, Q. Su, C. Zheng, Y. Zhang, Y. Wang, D. Guo, Y. He, Y. Zhu, Emission characteristics of filterable particulate matter and condensable particulate matter from coal-fired power plants, Case Stud. Therm. Eng. 35 (2022) 102145, https://doi.org/10.1016/j.csite.2022.102145.
[40] C.-W. Yoon, M.-J. Kim, Y.-S. Park, T.-W. Jeon, M.-Y. Lee, A review of medical waste Management Systems in the Republic of Korea for hospital and medical waste generated from the COVID-19 pandemic, Sustainability 14 (6) (2022) 3678, https://doi.org/10.3390/su14063678.
[41] S. Yu, H. Dong, Uncover cost-benefit disparity of municipal solid waste incineration in Chinese provinces, Sustainability 12 (2) (2020) 697, https://doi.org/10.3390/su12020697.
[42] X. Yu, Y. Shi, T. Wang, X. Sun, Dust-concentration measurement based on Mie scattering of a laser beam, PLoS One 12 (8) (2017) e0181575, https://doi.org/10.1371/journal.pone.0181575.
[43] K. Zhang, Y. Peng, H. Yu, P. Ning, X. Hou, L. Zhu, S. Lu, The influence of concentration and size on the error of particulate matter detection using charge induction method, Atmos. Pollut. Res. 15 (11) (2024) 102254, https://doi.org/10.1016/j.apr.2024.102254.
[44] L. Zhang, X. Bi, J.R. Grace, Measurements of electrostatic charging of powder mixtures in a free-fall test device, Procedia Engineering 102 (2015) 295–304, https://doi.org/10.1016/j.proeng.2015.01.146.
[45] C. Zheng, D. Duan, Q. Chang, S. Liu, Z. Yang, X. Liu, W. Weng, X. Gao, Experiments on enhancing the particle charging performance of an electrostatic precipitator, Aerosol Air Qual. Res. 19 (6) (2019) 1411–1420, https://doi.org/10.4209/aaqr.2018.11.0400.
[46] X. Zheng, R. Zhang, H. Huang, Theoretical modeling of relative humidity on contact electrification of sand particles, Sci. Rep. 4 (1) (2014) 4399, https://doi.org/10.1038/srep04399.